IL NUOVO CIMENTO **49 C** (2026) 68
DOI 10.1393/ncc/i2026-26068-5

Colloquia: IFAE 2025

Tracks of new physics: Calibration of the $\mathrm{d}E/\mathrm{d}x$ measured at the ATLAS experiment looking for long-lived particles(*)

S. Ravera

INFN & Università di Genova - Genova - Italy

received 10 October 2025

Summary. — The ATLAS experiment, operating at the LHC at CERN in Geneva, is searching for new physics beyond the Standard Model. Long-Lived charged Particles (LLP) are one of the possible hypotheses of new physics. In particular, heavy-charged LLPs could be identified as they would travel much more slowly than the speed of light ($\beta < 1$), implying anomalous high specific ionisation energy losses ($\mathrm{d}E/\mathrm{d}x$), significantly greater than those of Standard Model particles. The $\mathrm{d}E/\mathrm{d}x$ of the LLP track can be measured using the ATLAS Pixel detector; its value is affected by the reduction of the pixel sensors' charge collection efficiency due to the radiation damage from LHC collisions. It is therefore necessary to calibrate this variable to equalise the track $\mathrm{d}E/\mathrm{d}x$ measurements throughout the entire data-taking period. This paper presents the results of the track $\mathrm{d}E/\mathrm{d}x$ calibration performed for the first time by normalising the $\mathrm{d}E/\mathrm{d}x$ value at the cluster level before evaluating the track $\mathrm{d}E/\mathrm{d}x$. Results are shown for the entire ATLAS Run 2 dataset and part of the Run 3 datasets (2022-2024).

1. – Introduction

The Large Hadron Collider (LHC) [1] at CERN in Geneva has been colliding protons and heavy ions since a decade allowing the ATLAS Experiment [2] (A Toroidal LHC ApparatuS), together with the CMS Experiment (Compact Muon Solenoid), to discover the of Higgs boson, study its properties and other Standard Model processes. In addition to these measurements, the ATLAS detector is also used to search for new physics beyond the Standard Model. One example of such studies is the search for Long-Lived charged Particles (LLP). In particular, heavy-charged LLPs could be identified as they would travel much more slowly than the speed of light ($\beta < 1$), implying anomalous high specific ionisation energy losses ($\mathrm{d}E/\mathrm{d}x$), significantly greater than those of Standard Model particles typically reconstructed by the detector. The measurement of $\mathrm{d}E/\mathrm{d}x$ in the pixel detector layers provides sensitivity to particles within the range $0.3 < \beta\gamma < 0.8$. Moreover, the specific ionisation associated with a track is also used in other areas, such as beauty physics or the identification of tracks from particles that are very close together in jets.

(*) IFAE 2025 - "New Technologies" session

2. – Measuring $\mathrm{d}E/\mathrm{d}x$ with the ATLAS Pixel detector

The ATLAS detector is a general-purpose detector with a forward-backwards symmetric cylindrical layout covering nearly 4π in solid angle [2]. It consists of an inner detector (ID) tracking system, to measure the trajectories of charged particles, surrounded by a 2 T solenoid, followed by calorimeters to measure the energy of particles, and a muon spectrometer (MS) inside toroidal magnets to provide additional tracking for muons. The detector is hermetic within its η acceptance and can therefore measure the missing transverse momentum (p_T, with magnitude E_T) associated with each event. A two-level trigger system is used to select events [3]. The ID is made of three detector systems organised in concentric regions covering $|\eta|$ <2.5. The outermost system (TRT) is composed of densely packed 4-mm-diameter cylindrical drift tubes, followed at a smaller radius by silicon micro-strip detectors (SCT). A silicon pixel detector covers the innermost region [4,5], which, being crucial for this paper, is described below in some detail.

The pixel detector is made of hybrid pixel module loaded on carbon supports. Staves have been used for the barrel, made by four concentric layers (IBL, B-Layer (BL), Layer-1 (L1) and Layer-2 (L2)), at radial distances of 3.4 cm to 13 cm from the LHC beam line; while disk-shaped supports built the end-caps (three disks per side). It can therefore provide, on average, four precision measurements for each track. The front-end electronics of the pixel modules allow the measurement of time-over-threshold (ToT), *i.e.*, the time interval with the signal above a preset threshold, which is digitised and recorded to 8 bits (4 bits for the IBL). The ToT is approximately proportional to the ionisation charge [6] and thus the specific ionisation of a charged particle track to be calculated. Compared to the other layers, the IBL has faster electronics but provides charge measurements with lower resolution and dynamic range. If the charge released in a pixel exceeds the IBL dynamic range (which is set at approximately 30000 electrons), an overflow bit (OF1) is set. The overflow mechanism is not present in the outer pixel layers, and hits exceeding the dynamic range (∼200000 electrons) are lost. The presence of an IBL overflow bit is due to a high specific-ionisation charge deposited locally in the sensor: the overflow may be due to nearby or low-momentum tracks, or to hadronic interactions. However, it may also be associated with a low beta gamma LLP crossing the detector. Therefore, as described in the next section, tracks with an IBL overflow bit undergo a dedicated analysis treatment [3].

3. – The $\mathrm{d}E/\mathrm{d}x$ as a mass estimator

The charge released by a track crossing the pixel detector is rarely contained within just one pixel; neighbouring pixels registering hits are joined together using a connected component analysis to form clusters [7]. The charge of a cluster is calculated by summing the charges of all pixels belonging to the cluster after calibration corrections. The $\mathrm{d}E/\mathrm{d}x$ measurement assigned to each track is then calculated by averaging the ionisation measurements (charge collected in the cluster per unit track length in the sensor, $\mathrm{d}E/\mathrm{d}x$) of its individual clusters. The specific ionisation follows a Landau distribution, and to reduce the effect of the tails of this distribution a truncated average ($\langle \mathrm{d}E/\mathrm{d}x \rangle_{trunc}$) is evaluated after removing the highest $\mathrm{d}E/\mathrm{d}x$ cluster, or the two highest $\mathrm{d}E/\mathrm{d}x$ clusters in the rare case of more than four pixel clusters on a track. Clusters including pixels at the sensor edges are dropped, as part of the charge may escape detection. The OF1 clusters are never used to calculate the $\langle \mathrm{d}E/\mathrm{d}x \rangle_{trunc}$, as their $\mathrm{d}E/\mathrm{d}x$ is only known to be above

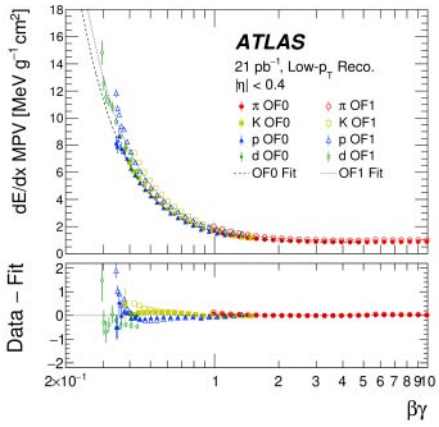

Fig. 1. – MPV values of $\langle \mathrm{d}E/\mathrm{d}x \rangle_{trunc}$ as a function of particle $\beta\gamma$ in $|\eta| < 0.4$, classified by IBL in overflow state (OF1) or not (OF0). The data values are fitted by a function reflecting the Bethe-Bloch formula [3].

a given value. Tracks for which the $\langle \mathrm{d}E/\mathrm{d}x \rangle_{trunc}$ is calculated using at least two clusters after removal of those meeting the criteria defined above are used for LLP searches, making this variable more robust against statistical fluctuations. Once the $\langle \mathrm{d}E/\mathrm{d}x \rangle_{trunc}$ is corrected for variations of the pixel detector conditions during the data-taking period, as described in detail in the next section, it can be used for new particle searches by calculating the $\beta\gamma$ of the crossing particle using the Bethe-Bloch relation and assuming charged particles to be charged pions by default, with unbiased reconstructed momentum [3]. A meaningful $\beta\gamma$ value can only be estimated in the range $0.3 < \beta\gamma < 0.8$ using the pixel detector. The lower limit is a consequence of the ToT dynamic range, while the upper limit is due to the proximity of the MIP regime, which begins at $\beta\gamma \simeq 3$ and where the dE/dx measurement becomes quasi-independent of $\beta\gamma$. Note that a dedicated low-pileup dataset is used for the dE/dx-to-$\beta\gamma$ calibration. In this dataset, thanks to the low vertices multiplicity, tracks are reconstructed if they have $p_T > 100$ MeV, while the minimum p_T requirement in the standard dataset is 500 MeV. An example of the 2017 calibration is shown in fig. 1.

4. – Motivations and strategy of the dE/dx equalisation

The charge collection efficiency decreases with increasing integrated luminosity received by the detector because of the damage induced in the silicon by the particle flux. The value of the $\langle \mathrm{d}E/\mathrm{d}x \rangle_{trunc}$ is therefore not constant over time. To use the value of $\langle \mathrm{d}E/\mathrm{d}x \rangle_{trunc}$ for LLPs searches, it must be constant over time, and then it needs to be equalised to a reference value. The reference value is calculated using the first fb^{-1} collected at the beginning of 2016 data-taking, when the detector was very little affected by radiation damage. While for the Run 2 datasets, the value of $\langle \mathrm{d}E/\mathrm{d}x \rangle_{trunc}$ was equalised to its reference value. The strategy for the Run 2 + Run 3 is different: the cluster dE/dx will be equalised to its reference value before calculating the $\langle \mathrm{d}E/\mathrm{d}x \rangle_{trunc}$. This is needed to cope with the complex η-layer dependencies of the radiation damage and avoid biasing the calculation of the $\langle \mathrm{d}E/\mathrm{d}x \rangle_{trunc}$: clusters of the outermost lay-

ers, measuring higher values of $\mathrm{d}E/\mathrm{d}x$, are most likely to be dropped. Special datasets where the cluster $\mathrm{d}E/\mathrm{d}x$ is saved have been produced using the Run 2 datasets (2015-2018) and part of the Run 3 dataset (2022-2024)(usually only the track $\mathrm{d}E/\mathrm{d}x$ is saved in the standard ATLAS datasets). To have enough statistics for the cluster equalisation, several ATLAS runs have been merged together to build samples with 1 fb^{-1} data. Moreover, pixel modules in the same layer, sharing the same longitudinal position on the local support, are grouped to make what we call an η-module-slice. The equalisation is then done by applying scale factors that are unique per each ATLAS run (w_{run}) and layer-η-module-slice ($\mathrm{w}^{layer}_{\eta-module-slice}$) to the cluster $\mathrm{d}E/\mathrm{d}x$, as shown in eq. (1):

$$\left\langle \frac{\mathrm{d}E}{\mathrm{d}x} \right\rangle_{corr} = w_{run} \sum_{i}^{N-n} \frac{(w^{layer}_{\eta-module-slice})^{i} (\mathrm{d}E/\mathrm{d}x)^{i}_{clust}}{N-n}. \tag{1}$$

Equation (1) shows the normalization of the track $\mathrm{d}E/\mathrm{d}x$, where N is the number of clusters, passing the selection described in sect. **4**, of each track, n is the number of rejected clusters per each track, w_{run} is the correction factor to be applied, unique per each run and $w^{layer}_{\eta-module-slice}$ is the correction factor to be applied based on the physical position if the module in the detector. Note that the scale factors are produced by normalising the Most Probable Value (MPV) of the $\mathrm{d}E/\mathrm{d}x$ distribution to its reference value. The MPV is obtained via a Landau-Gauss fit procedure with the fit range optimised around the peak of the distribution.

The η-module-slice scale factor is mainly aimed at correcting for the uniform radiation damage affecting the detector. As an example, fig. 2(left) shows that at central η (η-module-slice=0) after ∼380 fb^{-1} delivered by LHC at the end of 2024([1]), the MPV of the cluster $\mathrm{d}E/\mathrm{d}x$ is reduce by ∼50% in B-Layer, while only by ∼10% in Layer-2. On the same fig. 2(right) is clear the η dependence of the radiation damage: as an example the cluster $\mathrm{d}E/\mathrm{d}x$ of the outermost η-module-slice ((η-module-slice=6) in B-Layer is reduced only by ∼20% instead of the ∼50% in the central η-module-slice. Note that occasional jumps in the trend (*e.g.* at around 120 fb^{-1}) indicate changes to the Pixel detector main working point conditions, such as threshold and bias voltage, while smaller fluctuations correspond to regular retuning of the charge and threshold calibrations during machine development periods or technical shutdowns.

5. – Track $\mathrm{d}E/\mathrm{d}x$ equalised

The most probable value of the $\mathrm{d}E/\mathrm{d}x$ released by a charged particle intrinsically depends on the thickness of the material passed through [8]. This causes $\langle \mathrm{d}E/\mathrm{d}x \rangle_{trunc}$ to have a residual dependency on track-η, as it is shown in fig. 3(left) where the trend of the raw $\langle \mathrm{d}E/\mathrm{d}x \rangle_{trunc}$ is plotted for the entire dataset. Once again, it is clear that the effect of the radiation damage leads the $\langle \mathrm{d}E/\mathrm{d}x \rangle_{trunc}$ to be reduced by ∼40% after ∼380 fb^{-1}. The $\langle \mathrm{d}E/\mathrm{d}x \rangle_{trunc}$ can then be recomputed by applying the η-module-slice scale factors to the cluster $\mathrm{d}E/\mathrm{d}x$ leading to a significant equalisation as it is shown in fig. 3(right). Once the cluster $\mathrm{d}E/\mathrm{d}x$ has been corrected, there is still an η dependence in the value of the track $\langle \mathrm{d}E/\mathrm{d}x \rangle_{trunc}$. Therefore the final step of the equalization of the

([1]) Only tracks with transverse momentum ($\mathrm{p}_T > 1$ GeV, $|\mathrm{d}_0| < 1.5$ mm, no clusters shared with other tracks and at least 6 silicon hits (Pixel + SCT) have been selected.

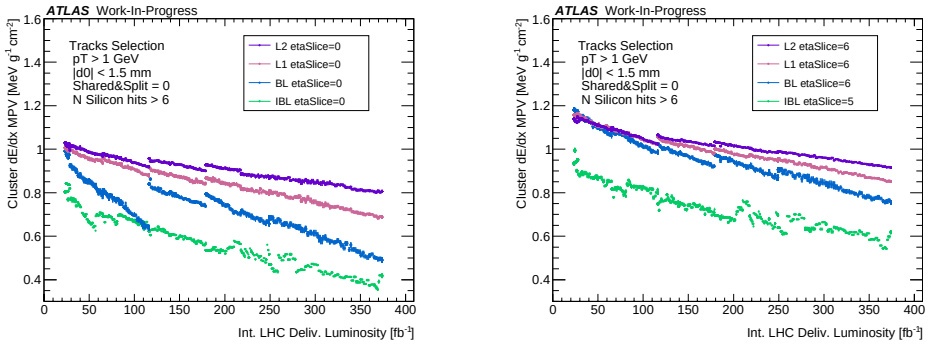

Fig. 2. – The drift of the clusters MPV for MIPs with $p_T < 1$GeV as a function of the LHC delivered integrated luminosity in Run 2 and Run 3 (up to 2024), for the central η-module-slice of the detector (left) and for the outermost η-module-slice of the detector (right). Note that only tracks where IBL is not in overflow state have been selected.

$\langle \mathrm{d}E/\mathrm{d}x \rangle_{trunc}$ is done by applying run specific scale factors (w_{run}), see eq. /1), sliced in ranges of track-η, to correct the residual dependence in track-η of the $\langle \mathrm{d}E/\mathrm{d}x \rangle_{trunc}$. The development of the tools to perform this final step of the equalisation is still ongoing, so it is not shown in this proceeding.

A further validation of the cluster dE/dx equalisation is obtained by studying the RMS of the clusters-on-track dE/dx. As it is shown in fig. 4(right) the value of RMS increases roughly by ∼90% at the end of 2024 (∼380 fb^{-1}). The increase of the RMS is then limited by ∼30% after applying the η-module-slice scale factors to the cluster dE/dx, as it is presented in fig. 4(right). Note that the residual increase in the value of the RMS after the cluster dE/dx may be related to other effects, such as the reduction of the cluster size.

6. – Conclusions

This study highlights the importance of a precise dE/dx calibration in the ATLAS Pixel detector for long-lived charged particle searches. Radiation damage from increas-

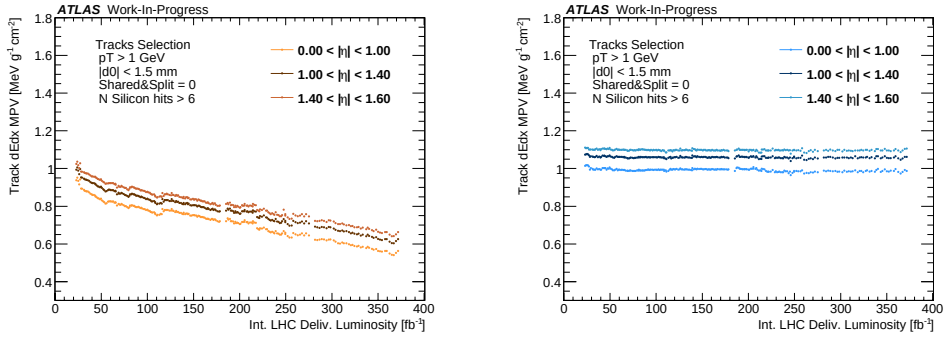

Fig. 3. – The drift of MIP-MPV raw $\langle \mathrm{d}E/\mathrm{d}x \rangle_{trunc}$ as a function of the delivered integrated luminosity in Run 2 and Run 3 (up to 2024) for different track-η ranges (left). The $\langle \mathrm{d}E/\mathrm{d}x \rangle_{trunc}$ is then recomputed applying the η-module-slice scale factors at cluster level (right).

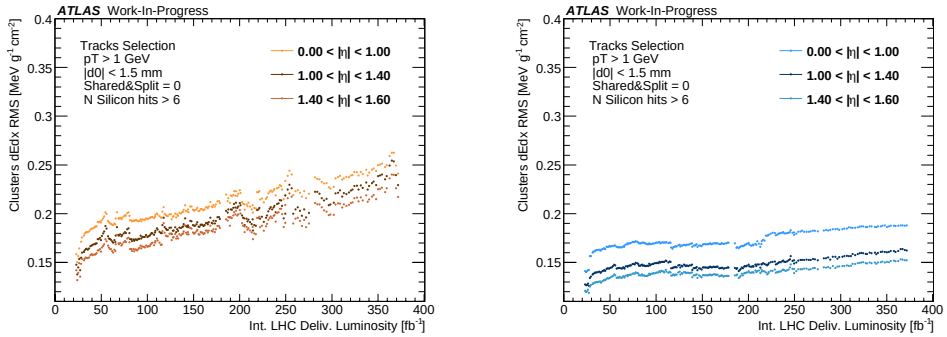

Fig. 4. – The drift of the RMS of the good clusters $\mathrm{d}E/\mathrm{d}x$ used to evaluate the raw $\langle \mathrm{d}E/\mathrm{d}x \rangle_{trunc}$ as a function of the delivered integrated luminosity in Run 2 and Run 3 (up to 2024) for different track-η ranges (left) and the RMS recomputed applying the η-module-slice scale factors at cluster level (right).

ing luminosity degrades charge collection, introducing non-uniformities in the $\mathrm{d}E/\mathrm{d}x$ response. A correction method based on run conditions and detector geometry (η-module-slice) allows the equalisation of ionisation measurements to a reference. The improved uniformity in track $\mathrm{d}E/\mathrm{d}x$ confirms the method's effectiveness. This calibration is essential to preserve sensitivity to anomalous ionisation signatures, thus strengthening ATLAS's potential to discover long-lived particles.

REFERENCES

[1] Evans L. and Bryant P., *JINST*, **3** (2008) S08001.
[2] ATLAS Collaboration, *JINST*, **3** (2008) S08003.
[3] ATLAS Collaboration, *Search for heavy, long-lived, charged particles with large ionisation energy loss in pp collisions at* $\sqrt{s}$ *= 13 TeV using the ATLAS experiment and the full Run 2 dataset.*
[4] ATLAS Collaboration, *ATLAS pixel detector: Technical Design Report*, ATLAS-TDR-11, CERN, Geneva (1998).
[5] ATLAS Collaboration, *ATLAS Insertable B-Layer Technical Design Report*, CERN-LHCC-2010-013 (2010).
[6] BaBar Collaboration, *Nucl. Instrum. Methods A*, **479** (2002) 1, arXiv:hep-ex/0105044.
[7] ATLAS Collaboration, *JINST*, **9** (2014) P09009, arXiv:1406.7690.
[8] Particle Data Group (Workman R. L. *et al.*), *Prog. Theor. Exp. Phys.*, **2022** (2022) 083C01.